Articles in PresS. Am J Physiol Renal Physiol (March 8, 2017). doi:10.1152/ajprenal.00671.2016

Nitric Oxide Reduces Paracellular Resistance in Rat Thick Ascending Limbs by Increasing Na^+ and Cl^- Permeabilities

Casandra M. Monzon[1,2], Rossana Occhipinti[1], Omar P Pignataro[2,3], Jeffrey L. Garvin[1]

[1]Department of Physiology and Biophysics. Case Western Reserve University. Cleveland, OH.

[2]Departamento de Química Biológica, FCEN-UBA. Buenos Aires, Argentina.

[3]Laboratorio de Endocrinología Molecular y Transducción de Señales, Instituto de Biología y Medicina Experimental, Consejo Nacional de Investigaciones Científicas y Técnicas (CONICET), Buenos Aires, Argentina.

Corresponding author:

Casandra Monzon

Case Western Reserve University

Department of Physiology and Biophysics

Robbins E532

10900 Euclid Avenue, MS 4970

Cleveland, OH 44106-4970

Phone: (216) 368-1687 Fax: (216) 368-5586

E-mail: casandra.monzon@case.edu

Short title: NO reduces thick ascending limb paracellular resistance

Abstract:

About 50% of the Na^+ reabsorbed in thick ascending limbs traverses the paracellular pathway. Nitric oxide (NO) reduces the permselectivity of this pathway via cGMP, but its effects on absolute Na^+ (P_{Na}^+) and Cl^- (P_{Cl}^-) permeabilities are unknown. To address this, we measured the effect L-arginine (0.5mmol/L; NO synthase substrate) and cGMP (0.5mmol/L) on P_{Na}^+ and P_{Cl}^- calculated from the transepithelial resistance (Rt) and P_{Na}^+/P_{Cl}^- in medullary thick ascending limbs. Rt was 7722±1554 ohm-cm in the control period and 6318±1757 ohm-cm after L-arginine treatment ($p<0.05$). P_{Na}^+/P_{Cl}^- was 2.0±0.2 in the control period and 1.7±0.1 after L-arginine ($p<0.04$). Calculated P_{Na}^+ and P_{Cl}^- were 3.52±0.2 $x10^{-5}$ cm/sec and 1.81±0.10 $x10^{-5}$ cm/sec respectively in the control period. After L-arginine they were 6.65±0.69 $x10^{-5}$ cm/sec ($p<0.0001$ vs control) and 3.97±0.44 $x10^{-5}$ cm/sec ($p<0.0001$), respectively. NOS inhibition with L-NAME (5mmol/L) prevented L-arginine's effect on Rt. Next we tested the effect of cGMP. Rt in the control period was 7592±1470 ohm-cm and 4796±847 ohm-cm after dibutyryl-cGMP (0.5mmol/L; db-cGMP) treatment ($p<0.04$). P_{Na}^+/P_{Cl}^- was 1.8±0.1 in the control period and 1.6±0.1 after db-cGMP ($p<0.03$). P_{Na}^+ and P_{Cl}^- were 4.58±0.80 $x10^{-5}$ cm/sec and 2.66±0.57 $x10^{-5}$ cm/sec, respectively, for the control period, and 9.48±1.63 $x10^{-5}$ cm/sec ($p<0.007$) and 6.01±1.05 $x10^{-5}$ cm/sec ($p<0.005$), respectively, after db-cGMP. We modeled NO's effect on luminal Na^+ concentration along the thick ascending limb. We found that NO's effect on the paracellular pathway reduces net Na^+ reabsorption, and that the magnitude of this effect is similar to that due to NO's inhibition of transcellular transport.

Keywords: sodium transport, nitric oxide, paracellular permeability, kidney

Introduction

As a diluting segment, the thick ascending limb reabsorbs solutes but little or no water. Net NaCl reabsorption in this portion of the nephron accounts for ~30% of the NaCl load filtered by the glomerulus (3). About half of the Na^+ is reabsorbed through active, transcellular transport. The remainder, and other cations, are reabsorbed via the paracellular pathway, or shunt, due to the lumen-positive voltage created as a consequence of active transport (13, 15). The route through the tight junctions of neighbor cells is markedly cation selective in thick ascending limbs with a Na^+/Cl^- permeability ratio (P_{Na}^+/P_{Cl}^-) of ~2 (5, 11, 15).

NO regulates salt and water reabsorption throughout the nephron (6, 17, 26, 27, 32). It is synthesized by nitric oxide synthase (NOS) from its substrate L-arginine. All three NOS isoforms (neuronal, inducible and endothelial) are expressed in mammalian thick ascending limbs. NO reduces the activity of transporters in the luminal membrane and thereby transepithelial NaCl and $NaHCO_3$ reabsorption (7, 9, 31, 33, 34). We previously showed that NO decreases the P_{Na}^+/P_{Cl}^- of the paracellular pathway in thick ascending limbs via cGMP (30). However, whether this is a result of a decrease in P_{Na}^+, an increase in P_{Cl}^-, or a simultaneous change in both P_{Na}^+ and P_{Cl}^- in opposite directions, and how these changes alter net salt reabsorption, is still unknown.

To calculate absolute permeabilities, one must know the transepithelial resistance (Rt) which is a measure of the hinderance encountered by ions traversing an epithelia through both trans- and paracellular conductive pathways. In thick ascending limbs Rt -or its inverse conductance- is predominantly a reflection of the ionic

permeability of the paracellular pathway, determined by the barrier function of the tight junctions(10, 12, 40). Changes in these variables can affect net solute transport. Rt of rat thick ascending limbs has not been reported nor has the effect of endogenously produced NO on this parameter.

The objective of this study was to evaluate the effects of NO on a) thick ascending limb Rt; b) the mechanism of action; c) the absolute permeabilities of both Na^+ and Cl^-; and d) how it impacts net Na^+ reabsorption.

Materials and Methods

Chemicals and solutions: Tubules were perfused and bathed with physiological saline, containing (in mmol/L): 130 NaCl, 4 KCl, 2.5 NaH_2PO_4, 1.2 $MgSO_4$, 6 L-alanine, 1 Na_3citrate, 5.5 glucose, 2 Ca(lactate)$_2$, and 10 4-(2-hydroxyethyl)-1-piperazine ethanesulfonic acid (HEPES), pH 7.4 at 37°C, unless otherwise stated. The final concentration of Na^+ and Cl^- was 142 and 134 mmol/L respectively. L-arginine, the substrate for NO production, and the NOS inhibitor N_ω-Nitro-L-arginine methyl ester hydrochloride, L-NAME, were obtained from Sigma-Aldrich (Milwaukee, WI). Dibutyryl-cGMP (db-cGMP) was from Enzo Life Sciences (Farmingdale, NY).

Animals: All protocols requiring animals were approved by the Institutional Animal Care and Use Committee of Case Western Reserve University in accordance with the National Institutes of Health Guide for the Care and Use of Laboratory Animals. Male Sprague-Dawley rats weighing 120-150gr (Charles River Laboratories, Wilmington, MA) were maintained on a diet containing 0.24% sodium and 1.1% potassium (Purina, Richmond, IN) for at least 4 days before use.

Isolation and Perfusion of Thick Ascending Limbs. Animals were anesthetized with ketamine and xylazine (100 and 20 mg/kg i.p. body weight, respectively). An abdominal incision was made, and the left kidney was removed and bathed in ice-cold physiological saline. The capsule was removed and coronal slices were cut. Thick ascending limbs were dissected from the outer medulla under a stereomicroscope at 4–10°C and placed in a temperature-regulated chamber (37 ± 1°C) with a flowing bath (1 ml/min). Tubules were perfused as described (4, 8).

Measurement of Rt. Prior to the experiment the injection artifact of the system was assessed by injecting current pulses of ±100 nA for 1 s four times in absence of the tubule. This procedure was also repeated at the end of the experiment after the tubule was released. Voltage deflections resulting from pulse injections were measured with three calomel electrodes and 150mM NaCl, 4% agar bridges connected to two electrometers in contact with the perfusion (Axoprobe 1A, Axon Instruments) and collecting pipettes, (Neuroprobe Amplifier, A-M Systems) and bath which was grounded. Values were recorded with a PowerLab acquisition system and PowerChart8 software (AD Instruments, Colorado Springs, CO). To measure Rt, isolated tubules were transferred to the chamber, bathed and perfused with physiological saline. After a 14-min equilibration period, current pulses were injected (±100 nA) over a minute under control conditions. Following, the test compound was added to the bath, a 15-min incubation period was allowed, and the injection procedure was repeated. The baseline voltage and the artifact of injection were subtracted from the mean voltage deflection caused by the current pulses to obtain the corrected voltage deflections for each period.

The corrected voltages were used to calculate the Rt for each period using cable analysis, as follows,

$$\frac{L}{\lambda} = \cosh^{-1}\left(\frac{V_0}{V_1}\right),$$

$$R_t = \frac{V_0 \lambda}{I_0} \tanh\left(\frac{L}{\lambda}\right)$$

Where: L (length of tubule); λ (space constant); V_o (voltage registered at proximal end); V_1 (voltage registered at distal end); R_t ; I_0 (current injected at proximal end). Results were expressed as specific Rt, which is the Rt normalized to unit length.

Measurement of Dilution Potentials and Calculation of P_{Na}^+/P_{Cl}^-. Tubules were initially bathed and perfused in symmetrical physiological saline for a 15-min equilibration period. Transepithelial voltage was measured with two calomel electrodes and 150mM NaCl, 4% agar bridges connected to an electrometer in contact with the perfusion pipette (Axoprobe 1A, Axon Instruments) and bath which was grounded. Voltages were recorded as described for Rt experiments. Thick ascending limbs were then bathed for an additional 6 min, and basal voltages were recorded during the last minute of this period. The bath was then changed to a solution based on physiologic saline in which Na^+/Cl^- were reduced to 32/24 mmol/L respectively (all other compounds in the solution remained the same) for 6 min. The osmolality was maintained at 290 mOsmol/kg using mannitol. The resulting difference in transepithelial voltage measured 1 min after the

exchange was considered the dilution potential of the control period. The bath was then restored to physiological saline for 12 min to allow tubules to recover. L-arginine (0.5 mmol/L), dibutyryl cGMP (100 umol/L) or vehicle was then added to the bath. Twenty min later the process was repeated in the presence of test compounds as indicated in the text. When L-nitroarginine methylester (L-NAME: 5 mmol/L) was used to inhibit NO synthesis, it was present from the beginning of the experiment. All dilution potentials were corrected for liquid junction potentials. P_{Na^+}/P_{Cl^-} values were calculated from dilution potentials using the Goldman-Hodgkin-Katz equation as we have done previously (30).

Calculation of Absolute Permeabilities. From the Rt values and P_{Na^+}/P_{Cl^-} , we calculated absolute P_{Na^+} and P_{Cl^-} with the Kimizuka-Koketsu equation (18, 19):

$$P_{Na^+} = \frac{G\left(\frac{RT}{F^2}\right)}{\alpha(1+\beta)},$$

$$P_{Cl^-} = P_{Na^+}\beta$$

Where: P_{Na^+} and P_{Cl}: Na^+ and Cl^- permeability; G: specific conductance, the inverse of specific Rt; R: ideal gas constant; T: temperature in degrees Kelvin; F: Faraday's constant; α: NaCl concentration; β: P_{Cl^-}/P_{Na^+}.

Mathematical Modeling of Luminal Na^+ Concentration Along the Thick Ascending Limb. A simple mathematical model of the luminal Na^+ concentration, $[Na^+]_i$, along the thick

ascending limb was developed following the approach of Layton et al (21) and Layton and Edwards (20). The model assumed that: a) the thick ascending limb is rigid extending from the bottom of the outer medulla (x = 0) to the top of the cortex (x = L) and the cortical-medullary junction is located at x = x^*; b) x is positive in the direction of the constant fluid flow Q along the tubule; c) the amount of Na^+ in the lumen ($Q \cdot [Na^+]_i$) changes along the tubule because of the rate of Na^+ reabsorption (J). Thus, the solute conservation equation for luminal $[Na^+]_i$ along the thick ascending limb at steady-state is given by the first-order ordinary differential equation (ODE)

$$Q\frac{d}{dx}([\mathrm{Na}^+]_\mathrm{i}) = -2\pi r \cdot J, \tag{1}$$

where r is the radius of the tubule (21). Because J depends on: 1) active transcellular transport (J_A) mediated by the apical Na^+-K^+-$2Cl^-$ cotransporter and the basolateral Na^+-K^+-ATPase; and 2) transport through the passive paracellular pathway (J_P) mediated by the lumen-positive voltage (V_m), it can be written that

$$J = J_\mathrm{A} + J_\mathrm{P}. \tag{2}$$

J_A follows Michaelis-Menten kinetics, that is

$$J_\mathrm{A} = T_\mathrm{max}\frac{[\mathrm{Na}^+]_\mathrm{i}}{K_m + [\mathrm{Na}^+]_\mathrm{i}}, \tag{3}$$

where the maximal velocity T_{max} is assumed to be 400 pmol/mm/min similar to what has been done previously (21). This yields a physiologically relevant $[Na^+]_i$ of ~25 mmol/L (2) at the end of the tubule. The value of K_m is 30 mmol/L, an average of the K_m for Cl^-. The average Km for Cl^- of the different NKCC2 isoforms present in the outer medulla

and cortex was used since: 1) it is an obligatory cotransported anion with Na^+ in thick ascending limbs; and 2) it is the rate limiting ion for transcellular Na^+ reabsorption.

J_P follows the Goldman-Hodgkin-Katz (GHK) equation

$$J_P = P_{Na^+} \frac{FV_m}{RT} \left(\frac{[Na^+]_i - [Na^+]_o \exp(-FV_m / RT)}{1 - \exp(-FV_m / RT)} \right), \quad (4)$$

where P_{Na^+} F, R and T have the same meanings as defined above. $[Na^+]_o$ is the interstitial $[Na^+]$. Because $[Na^+]_o$ depends on transport and J_A decays exponentially, $[Na^+]_o$ was assumed to decay exponentially from the initial interstitial $[Na^+]_{o,initial}$ (at x = 0) to the final interstitial $[Na^+]_{o,final}$ (at x = L), according to the equation

$$[Na^+]_o = ([Na^+]_{o,initial} - [Na^+]_{o,final}) \exp(-x / \tau) + [Na^+]_{o,final}. \quad (5)$$

Here, considering that outer medullary osmolality is approximately 350-400 mOsm/kg (16), $[Na^+]_{o,initial}$ was chosen to be 175 mmol/L. Cortical osmolality is 290 mOsm/kg and therefore the value of $[Na^+]_{o,final}$ was chosen to be 140 mmol/L. Moreover, because of the high perfusion rates in the cortex, $[Na^+]_o$ reaches its minimum value of 140 mmol/L (i.e., $[Na^+]_{o,final}$) at the cortical-medullary junction, (i.e., at $x = x^*$). The value of the rate constant τ, chosen to be 0.03, guarantees that $[Na^+]_o$ reaches its minimum value of 140 mmol/L at x* = 0.18 cm, 30% of the total tubular length L (0.6 cm) tubule .

Finally, because the lumen-positive voltage, V_m, is influenced by both the active and passive transport, it was written that

$$V_m = V_A + \alpha V_P. \quad (6)$$

Here, because the active component of the voltage, V_A, is due to the active transport J_A and because J_A follows Michaelis-Menten kinetics (see equation (3)), it was assumed that V_A also follows Michaelis-Menten kinetics according to the equation

$$V_A = V_{max} \frac{[Na^+]_i}{K_m + [Na^+]_i}, \quad (7)$$

with K_m same as in J_A, and V_{max} the maximal lumen positive voltage of 10 mV measured at the beginning of the tubule when J_A is at a maximum.

In equation (6) the passive component of the voltage, V_P, is given by the Nernst equation

$$V_P = 2.303 \frac{RT}{F} \log_{10}\left(\frac{[Na^+]_o}{[Na^+]_i}\right). \quad (8)$$

Alpha (α) is a factor used to correct the passive component of the transepithelial voltage, V_P. It corrects V_P to compensate for the fact that we are not accounting for the effect of Cl^- on V_P in our simple model. Thus, to obtain a "physiological voltage" due to the paracellular component one must multiply V_P by α. The total transepithelial voltage is then given by equation 6. α is calculated as the ratio between the membrane voltage predicted by the Goldman-Hodgkin-Katz (GHK) equation for both Na^+ and Cl^- ($V_{P,GHK}$) and by the Nernst equation for Na^+ only ($V_{P,Nernst}$). The Na^+ and Cl^- concentrations used to calculate the correction factor α were those used in the dilution potential experiments where $[Na^+]_{i,*}$ = 142 mmol/L, $[Na^+]_{o,*}$ = 32 mmol/L, $[Cl^-]_{i,*}$ = 134 mmol/L, and $[Cl^-]_{o,*}$ = 24 mmol/L.

That is,

$$\alpha = \frac{V_{P,GHK}}{V_{P,Nernst}} = \frac{2.303\frac{RT}{F}\log_{10}\left(\frac{P_{Na^+}[Na^+]_{o,*} + P_{Cl^-}[Cl^-]_{i,*}}{P_{Na^+}[Na^+]_{i,*} + P_{Cl^-}[Cl^-]_{o,*}}\right)}{2.303\frac{RT}{F}\log_{10}\left(\frac{[Na^+]_{o,*}}{[Na^+]_{i,*}}\right)}, \quad (9)$$

Assuming that $[Na^+]_i$ = 175 mmol/L at the beginning of the tubule (x = 0), r = 10 μm and Q = 10 nL/min, the above ODE (1) was solved in Matlab using the stiff ODE solver, ode15s.

Four simulations were performed to predict the luminal Na^+ concentration along the tubule under the following conditions: 1) control; 2) considering the effect of NO on the paracellular pathway only; 3) considering the effect of NO on the transcellular pathways only; 4) considering the effect of NO on both the paracellular and transcellular pathways combined. A control experiment was simulated by using the control P_{Na^+} and P_{Cl^-} values obtained in this study and the calculated α value for these conditions. Next, the effect of NO on the paracellular pathway only was simulated by assigning P_{Na^+} and P_{Cl^-} values calculated in the presence of L-arginine in this study, and the calculated α value for these conditions. The effect of NO on the transcellular pathway only was simulated by reducing the value of T_{max} by 30%, that is T_{max} = 280 pmol/mm/min, and by assigning P_{Na^+} and P_{Cl^-} values as in the control case and the calculated α value. Finally, the effect of NO on both the paracellular and transcellular pathway was simulated by reducing the value of T_{max} by 30% and by assigning to P_{Na^+}, P_{Cl^-} and α the same values used for the simulation in which we tested the effect of NO on the paracellular pathway only.

Statistical analysis: All data were analyzed with a two-tailed Student's t-test for paired experiments. Absolute permeabilities were calculated from P_{Na^+}/P_{Cl^-} and specific transepithelial resistances by "boot strapping". Results are presented as means ± SEM. A p value of <0.05 was considered significant.

Results

We first measured Rt and the effects of endogenously produced NO on this parameter as required to calculate absolute permeabilities of Na^+ and Cl^- in medullary thick ascending limbs, and the effects of NO. Additionally, these values have not been reported previously. Rt was measured by recording the voltage deflections at both proximal and distal ends of the tubule caused by current pulses in the absence or presence of L-arginine (0.5mmol/L). During the control period, the specific Rt was 7722 ±1554 ohm-cm and it was 6318 ± 1757 ohm-cm after adding L-arginine to stimulate NO production (Fig 1A, n=10, $p<0.05$).

To test whether the effect of L-arginine on Rt was due to NO, we studied the ability of L-nitromethylester (L-NAME), a NO synthase inhibitor, to block its effects. In the presence of L-NAME (5mmol/L), the specific Rt was 7924 ± 1964 ohm-cm. After addition of L-arginine in the presence of L-NAME, the specific Rt was 8463 ± 1725 ohm-cm, not significantly different from the value in the control period (Fig 1B, n=6). L-NAME alone did not affect Rt.

We next studied the effect of endogenous NO on dilution potentials and thus P_{Na^+}/P_{Cl^-}s because these values are required to calculate absolute Na^+ and Cl^- permeabilities. During the control period, the dilution potential was -11.0 ± 1.1 mV. After

adding L-arginine to the bath, the dilution potential was -9.0 ± 1.3 mV (Fig 2A, n=9, p< 0.05). The calculated P_{Na}^{+}/P_{Cl}^{-} was 2.0 ± 0.2 during the control period. After L-arginine it was 1.7 ± 0.1 (Fig 2B, p< 0.04).

Once we collected both P_{Na}^{+}/P_{Cl}^{-} values and Rt data, we calculated the absolute permeabilities for Na^{+} and Cl^{-}, and the effects of NO. During the control period calculated P_{Na}^{+} and P_{Cl}^{-} were 3.52 ± 0.21 x 10^{-5} cm/s and 1.81 ± 0.17 x 10^{-5} cm/s, respectively. After adding L-arginine to stimulate NO production, they increased to 6.65 ± 0.69 x 10^{-5} cm/s (p<0.0001 vs P_{Na}^{+} control) and 3.97 ± 0.44 x 10^{-5} cm/s (p<0.0001 vs P_{Cl}^{-} control), respectively (Fig 2C, n=50).

We then investigated the effect of the membrane-permeant cGMP analogue dibutyryl-cGMP (db-cGMP) on Rt in this segment. During the control period, the specific Rt was 7592 ± 1470 ohm-cm. After db-cGMP (0.5mmol/L) it was 4796 ± 847 ohm-cm (Fig 3, n=10, p<0.04).

We next studied the effect of db-cGMP on dilution potentials. During the control period, the dilution potential was -9.8 ±1.0 mV. After adding db-cGMP, the dilution potential was -7.5 ± 1.1 mV (Fig 4A, n=6, p<0.02). The calculated P_{Na}^{+}/P_{Cl}^{-} was 1.8 ± 0.1 during the control period and 1.6 ± 0.1 after db-cGMP treatment (Fig 4B, n=6, p<0.03).

Using the P_{Na}^{+}/P_{Cl}^{-} and Rts, we calculated the effects of db-cGMP on P_{Na}^{+} and P_{Cl}^{-} as for NO. During the control period, P_{Na}^{+} and P_{Cl}^{-} were 4.58 ± 0.80 x 10^{-5} cm/s and 2.66 ± 0.57 x 10^{-5} cm/s, respectively. After db-cGMP treatment they were 9.48 ± 1.63 x

10^{-5} cm/s ($p<0.007$ vs P_{Na}^{+} control) and 6.01 ± 1.05 x 10^{-5} cm/s ($p<0.005$ vs P_{Cl}^{-} control), respectively (Fig 4C, n=50).

The changes in permeabilities of Na^+ and Cl^- caused by NO could either blunt the inhibitory effect of NO on transcellular transport by increasing salt flux through the paracellular pathway or they could augment the inhibitory effect by reducing reabsorption via this route. To address this question, we designed a mathematical model to predict the effect of NO on luminal Na^+ concentration. Figure 5 shows the model's predictions as a function of tubular length. The solid black line represents the control conditions using an α value of 0.28 (the correction factor used to account for the effect of Cl^- as described in the Methods). The dashed line takes into account the effect of NO only on the paracellular pathway using an α value of 0.22. The blue line takes into account the effect of NO only on the transcellular pathway (blue line) using an α = 0.28. The green line takes into account the combined effects of NO on both the transcellular and paracellular pathways using an α value of 0.22. Under control conditions in the absence of NO luminal Na^+ falls exponentially to 22.4 mmol/L by the end of the thick ascending limb. When only the effect of NO on the paracellular pathway was considered, Na^+ reabsorption was augmented early in the thick ascending limb but by the end of the tubule the Na^+ concentration was 33.9 mmol/L, much greater than the control condition. The same was true when considering the effect of NO on the transcellular pathway only, which results in a luminal concentration of Na^+ at the end of the tubule of 46.2 mmol/L. When the effects of NO on both transcellular and paracellular pathways were included in the model, the luminal Na^+ concentration was always greater than control, and by the end of the tubule was 52.5 mmol/L.

Discussion

The objective of this work was to investigate the effect of NO on the paracellular pathway of thick ascending limbs and its impact on net Na^+ reabsorption. We found that: 1) endogenously produced NO decreases Rt; 2) inhibition of NOS prevents the decrease in Rt; 3) NO reduces P_{Na}^+/P_{Cl}^- in thick ascending limbs; 4) NO increases absolute P_{Na}^+ and P_{Cl}^-, but the increase of P_{Cl}^- is greater; 5) cGMP mimics the effects of NO on P_{Na}^+/P_{Cl}^-, Rt, P_{Na}^+ and P_{Cl}^-; 6) the effects of NO on the paracellular pathway reduce Na^+ reabsorption ; and 7) the contributions of NO-induced inhibition of paracellular and transcellular Na^+ reabsorption to the reduction in net Na^+ transport are equal.

We first studied the effect of NO on Rt, which assesses predominantly paracellular permeability to ions in this segment(10). Rt in rat thick ascending limbs and the effects of NO have not been reported previously. We found that the specific Rt was about 7700 ohm-cm (~46 ohm-cm^2) during the control period and that it decreased when L-arginine, the substrate for NO production, was added. This effect was blocked by the NOS inhibitor L-NAME. These results show that NO induces changes in the barrier function of the tight junctions.

We next studied the effect of NO on P_{Na}^+/P_{Cl}^-, an indicator of paracellular permselectivity, which was calculated from Na^+/Cl^- dilution potentials. Dilution potentials arise from the movement of ions through the tight junctions down their concentration gradient which is dependent on the charge/size selectivity of the paracellular space. We found a P_{Na}^+/P_{Cl}^- of 2 during the control period while in the presence of NO, P_{Na}^+/P_{Cl}^-

decreased to about 1.7. These data indicate that NO regulates the relative P_{Na}^{+} and P_{Cl}^{-} differently. However, this ratio alone does not provide information of how the absolute, individual permeabilities are affected by NO.

With both Rt and P_{Na}^{+}/P_{Cl}^{-} values, we calculated the absolute permeabilities for Na^{+} and Cl^{-}. We found that NO increased both P_{Na}^{+} and P_{Cl}^{-}, but P_{Cl}^{-} increased more. These are the first data showing that NO has an effect on absolute P_{Na}^{+} and P_{Cl}^{-} in any nephron segment. Because NO increases P_{Cl}^{-} more than P_{Na}^{+}, the effects of NO on the paracellular pathway likely further reduce the lumen positive potential normally generated in thick ascending limbs by active transport.

c-GMP mediates most of the effects of NO. Thus we tested the effect of this signaling molecule on Rt and P_{Na}^{+}/P_{Cl}^{-}. c-GMP caused a decrease in Rt, and an increase in both P_{Na}^{+} and P_{Cl}^{-} comparable to those evoked by NO. These data suggest that the second messenger mediating the final effect of NO on Rt, absolute permeabilities, and possibly solute reabsorption via the paracellular pathway is c-GMP.

Finally, we used a simple mathematical model to investigate the effect of NO on luminal Na^{+} concentration along the length of the thick ascending limb based on our results. Early in the tubule, at the deepest point in the outer medulla, the model predicts lower luminal Na^{+} concentrations (indicating that more Na^{+} is reabsorbed) when the effect of NO on only the paracellular pathway but not active transcellular transport is considered compared to control. This is due to high rates of transcellular transport creating a large lumen positive voltage but still a relatively small transepithelial Na^{+} gradient and the increase in permeability caused by NO. However by the end of the thick ascending limb in the cortex, the model predicts a greater luminal Na^{+}

concentration (indicating that less Na^+ is reabsorbed) in the presence of NO than its absence. This is due to 1) active transport creating a large transepithelial Na^+ gradient favoring Na^+ entry into the lumen from the interstitium, i.e. back flux; 2) the increase in paracellular permeability caused by NO and 3) the reduction in P_{Na^+}/P_{Cl^-} which diminishes the lumen-positive potential. Figures 6 and 7 show plots for J_P and V_m (and its components V_A and $\alpha*V_P$) along the length of the tubule. Although backflux is evident under control conditions and when the effects of NO on transcellular transport alone, the paracellular pathway alone and both the transcellular and paracellular pathway are taken into account, when analyzing J_P backflux begins earlier in the tubule and is more pronounced throughout the remainder of the tubule when the effect of NO only on J_P is taken into account. This is consistent with the reduction in P_{Na^+}/P_{Cl^-}.

When the effects of NO on both the paracellular pathway and active transcellular transport are considered the results are somewhat different. Now, the luminal Na^+ concentration in the presence of NO is always greater along the tubule when compared to the control condition. This is due to several factors including: 1) the direct inhibition of active transport; 2) a reduction in the lumen positive voltage which diminishes part of the driving force for Na^+ reabsorption via the paracellular pathway; and 3) the increase in paracellular pathway permeability which allows a larger back flux of Na^+ from the interstitium into the lumen. Although the effect of NO on each pathway analyzed individually shows an inhibitory effect on Na^+ reabsorption leading to a higher luminal Na^+ concentration at the end of the tubule, they are antagonistic with the combined action being less than the sum of the individual effects.

One important caveat of the model is that we have assumed that NO has the same effect on trans- and paracellular transport in both medullary and cortical thick ascending limbs. This may or may not be a completely valid assumption because the effects of NO have not been studied on cortical thick ascending limb salt reabsorption to our knowledge and cortical and medullary thick ascending limbs respond differently to some regulatory factors.

In our experiments we assumed that the change in Rt observed in the presence of NO was primarily due to changes in paracellular ionic permeability rather than to specific transcellular resistance. This assumption is supported by several lines of evidence. First, P_{Na^+}/P_{Cl^-} was reduced by NO. This can only occur due to a change in the paracellular pathway since there is no Na^+ or Cl^- conductance in thick ascending limb luminal membranes. To date, no one has reported the effects of NO on Rt or specific transcellular and paracellular resistance individually. We have shown previously that within the time frame of the current experiments NO does not alter Na^+/K^+-ATPase activity (38).

There is one report by Wu et al. of an inhibitory effect of NO on the 10 pS Cl^- channel in mouse cortical thick ascending limbs. However, our studies were performed in medullary thick ascending limbs and Winters et al. (41) reported a 80 rather than a 10 pS Cl^- channel in medullary thick ascending limbs. As a result it is not clear whether inhibition of the 10 pS Cl^- channel by NO is relevant to our study. Furthermore, while the 7-9 pS Cl- channel may be the most abundant in terms of numbers, it only carries slightly more current than 45 pS channel when factors such as single channel conductance, open probability, etc, are taken into account. These data suggest that the

effect of NO on the 10 pS channel may be not critically important to the overall resistance measurement.

There is some evidence that NO stimulates luminal membrane rectified K^+ channels (ROMK) in rat thick ascending limbs (25, 39). If NO had both a stimulatory effect on ROMK and inhibitory effect on 10 pS Cl- channels as discussed above and we took them into account, they would nearly cancel each other out resulting in a very small quantitative change in our results.

The Rt values reported in the literature for the thick ascending limb range between 11-50 ohm cm^2 in mouse (14) and ~24-35 ohm cm^2 (5, 11) in rabbit. The Rt calculated in our experiments falls within these values. The difference between mouse and rat Rt values in this segment could reflect true species differences or be due to the use of varying techniques used to calculate Rt.

In our experimental design, P_{Na}^+/P_{Cl}^- values calculated from dilution potential experiments reflect the permselectivity of the paracellular pathway. In these experiments we reduced bath NaCl, and not the luminal solution. Thus active transcellular NaCl transport was not significantly changed by the solution switch. The value of 2 found in the control period is in accordance with that described in the literature for thick ascending limbs, and indicates that the paracellular pathway is twice as selective to Na^+ than it is for Cl^- (5, 11, 15). The reduction to 1.7 by NO is similar to what we have previously reported (30). Increasing evidence shows that the paracellular permselectivity is determined by claudin proteins in the tight junctions of epithelial tissues. The thick ascending limbs express claudin-3, -10, -11, -16 and -19 (1, 43). Some reports indicate that NO can interact with claudin proteins, and regulate their

expression/function in other systems (24, 28, 29), thus this could be occurring in our model.

We previously found that L-NAME inhibition of NOS has no effect on chloride reabsorption in isolated, perfused thick ascending limbs (35) due to our experimental conditions. We use L-arginine free solutions both in the lumen and the bath, so the L-arginine contained in the cell is transported out of the cell favored by its concentration gradient. Since the bath is continuously renewed, there is no L-arginine in our experimental design. Therefore, all protocols where the effect of endogenously-produced NO was evaluated required the addition of L-arginine. The exact concentration of L-arginine in the outer medulla has not been determined, but it has been reported to be ~0.5 mM in whole kidney (36), hence the concentration used in our experiments falls within the physiological range.

Our findings that NO regulates paracellular permeability are in agreement with a report by Liang et al (23). Using the NO donor nitroprusside, these authors found that NO caused an increase in ^{3}[H]-D-mannitol flux in OK cells, commonly used as an in vitro proximal tubule model. However, they did not measure the effects of nitroprusside on absolute P_{Na}^{+} and/or P_{Cl}^{-}. Similarly NO has been shown to increase paracellular permeability in non-renal epithelia. Data from Trischitta et al(37) suggest that NO modulates intestinal paracellular permeability by increasing conductance to ions. NO has also been shown to raise permeability by causing tight junction disassembly and gut barrier dysfunction (42).

We previously reported that the effects of NO on the permselectivity of the paracellular pathway in thick ascending limbs were mediated by c-GMP (30), but no

conclusion could be made at the time regarding its specific effect on the absolute permeabilities of Na^+ and Cl^-. Our novel finding that cGMP regulates P_{Na}^+ and P_{Cl}^- is supported by evidence in the literature. Trischitta et al showed that 8-br-cGMP, a cell membrane-permeable cGMP analog, reduced the dilution potential in eel intestine, suggesting that this second messenger could be decreasing P_{Na}^+, increasing P_{Cl}^-, or affecting both in different proportion/direction. Lee et al found that whereas 4 umol/L, 8-br-cGMP increased Rt in Sertoli cells, therefore promoting tight junction assembly, 0.1-1 mmol/L had the opposite effect. These data indicate that this second messenger has a biphasic effect where a low dose of cGMP lowers ionic permeability and a higher dose increases ionic permeability (22). It is not clear whether cGMP is part of the mechanism of action behind the effects of NO in OK cells by Liang (23). Incubation of the cells with a guanylate cyclase inhibitor did not prevent the increase in permeability but it also failed to abolish the increase in cGMP. Such results may indicate that the drug was not actually inhibiting cGMP production therefore no conclusion can be made.

In summary we have reported that: 1) Rt in rat thick ascending limbs is similar to that of other species; 2) NO reduces Rt; 3) NO increases absolute P_{Na}^+ and P_{Cl}^- in this segment; 4) these effects are mediated by c-GMP; and 5) perhaps most importantly, the effects of NO on the paracellular pathway reduce net Na^+ reabsorption in this segment. The results here presented contribute to a better understanding on the anti-hypertensive effects of NO.

Acknowledgements: None

Grants: This work was in part supported by grants from the National Institute of Health HL 028982 and HL070985 to J.G. and K01-DK107787 to R.O.

Disclosures: None

References

1. **Angelow S, El-Husseini R, Kanzawa SA, and Yu AS**. Renal localization and function of the tight junction protein, claudin-19. *American Journal of Physiology Renal Physiology* 293: F166-177, 2007.
2. **Bennett CM, Brenner BM, and Berliner RW**. Micropuncture study of nephron function in the rhesus monkey. *The Journal of Clinical Investigation* 47: 203-216, 1968.
3. **Burg M, and Good D**. Sodium chloride coupled transport in mammalian nephrons. *Annu Rev Physiol* 45: 533-547, 1983.
4. **Burg M, Grantham J, Abramow M, and Orloff J**. Preparation and study of fragments of single rabbit nephrons. *The American Journal of Physiology* 210: 1293-1298, 1966.
5. **Burg MB, and Green N**. Function of the thick ascending limb of Henle's loop. *The American Journal of Physiology* 224: 659-668, 1973.
6. **Gao Y, Stuart D, Pollock JS, Takahishi T, and Kohan DE**. Collecting duct-specific knockout of nitric oxide synthase 3 impairs water excretion in a sex-dependent manner. *American Journal of physiology Renal Physiology* 311: F1074-F1083, 2016.
7. **Garcia NH, Plato CF, Stoos BA, and Garvin JL**. Nitric oxide-induced inhibition of transport by thick ascending limbs from Dahl salt-sensitive rats. *Hypertension* 34: 508-513, 1999.
8. **Garvin JL, Burg MB, and Knepper MA**. Active NH4+ absorption by the thick ascending limb. *The American Journal of Physiology* 255: F57-65, 1988.
9. **Garvin JL, and Hong NJ**. Nitric oxide inhibits sodium/hydrogen exchange activity in the thick ascending limb. *The American Journal of Physiology* 277: F377-382, 1999.
10. **Gonzalez-Mariscal L, Chavez de Ramirez B, Lazaro A, and Cereijido M**. Establishment of tight junctions between cells from different animal species and different sealing capacities. *The Journal of Membrane Biology* 107: 43-56, 1989.
11. **Greger R**. Cation selectivity of the isolated perfused cortical thick ascending limb of Henle's loop of rabbit kidney. *Pflugers Archiv : European Journal of Physiology* 390: 30-37, 1981.
12. **Greger R**. Ion transport mechanisms in thick ascending limb of Henle's loop of mammalian nephron. *Physiological Reviews* 65: 760-797, 1985.
13. **Hebert SC, and Andreoli TE**. Ionic conductance pathways in the mouse medullary thick ascending limb of Henle. The paracellular pathway and electrogenic Cl- absorption. *The Journal of General Physiology* 87: 567-590, 1986.
14. **Hebert SC, Culpepper RM, and Andreoli TE**. NaCl Transport in Mouse Medullary Thick Ascending Limbs . 1. Functional Nephron Heterogeneity and Adh-Stimulated NaCl Cotransport. *The American Journal of Physiology* 241: F412-F431, 1981.
15. **Hebert SC, Culpepper RM, and Andreoli TE**. NaCl transport in mouse medullary thick ascending limbs. II. ADH enhancement of transcellular NaCl cotransport; origin of transepithelial voltage. *The American Journal of Physiology* 241: F432-442, 1981.
16. **Herrera M, and Garvin JL**. A high-salt diet stimulates thick ascending limb eNOS expression by raising medullary osmolality and increasing release of endothelin-1. *American Journal of Physiology Renal Physiology* 288: F58-64, 2005.
17. **Hyndman KA, Boesen EI, Elmarakby AA, Brands MW, Huang P, Kohan DE, Pollock DM, and Pollock JS**. Renal collecting duct NOS1 maintains fluid-electrolyte homeostasis and blood pressure. *Hypertension* 62: 91-98, 2013.
18. **Kahle KT, Macgregor GG, Wilson FH, Van Hoek AN, Brown D, Ardito T, Kashgarian M, Giebisch G, Hebert SC, Boulpaep EL, and Lifton RP**. Paracellular Cl- permeability is regulated by WNK4 kinase:

503 insight into normal physiology and hypertension. *Proceedings of the National Academy of Sciences of the*
504 *United States of America* 101: 14877-14882, 2004.
505 19. **Kimizuka H, and Koketsu K**. Ion transport through cell membrane. *J Theor Biol* 6: 290-305, 1964.
506 20. **Layton AT EA**. Mathematical Modeling in Renal Physiology. . 2014.
507 21. **Layton HE, Pitman EB, and Moore LC**. Bifurcation analysis of TGF-mediated oscillations in
508 SNGFR. *The American Journal of Physiology* 261: F904-919, 1991.
509 22. **Lee NP, and Cheng CY**. Regulation of Sertoli cell tight junction dynamics in the rat testis via the
510 nitric oxide synthase/soluble guanylate cyclase/3',5'-cyclic guanosine monophosphate/protein kinase G
511 signaling pathway: an in vitro study. *Endocrinology* 144: 3114-3129, 2003.
512 23. **Liang M, and Knox FG**. Nitric oxide enhances paracellular permeability of opossum kidney cells.
513 *Kidney International* 55: 2215-2223, 1999.
514 24. **Liu LB, Liu XB, Ma J, Liu YH, Li ZQ, Ma T, Zhao XH, Xi Z, and Xue YX**. Bradykinin increased the
515 permeability of BTB via NOS/NO/ZONAB-mediating down-regulation of claudin-5 and occludin.
516 *Biochemical and Biophysical Research Communications* 464: 118-125, 2015.
517 25. **Lu M, Wang X, and Wang W**. Nitric oxide increases the activity of the apical 70-pS K+ channel in
518 TAL of rat kidney. *The American Journal of Physiology* 274: F946-950, 1998.
519 26. **Majid DS, and Navar LG**. Nitric oxide in the control of renal hemodynamics and excretory
520 function. *American journal of hypertension* 14: 74S-82S, 2001.
521 27. **Manning RD, Jr., and Hu L**. Nitric oxide regulates renal hemodynamics and urinary sodium
522 excretion in dogs. *Hypertension* 23: 619-625, 1994.
523 28. **Merino-Gracia J, Costas-Insua C, Canales MA, and Rodriguez-Crespo I**. Insights into the C-
524 terminal Peptide Binding Specificity of the PDZ Domain of Neuronal Nitric-oxide Synthase:
525 CHARACTERIZATION OF THE INTERACTION WITH THE TIGHT JUNCTION PROTEIN CLAUDIN-3. *The Journal*
526 *of Biological Chemistry* 291: 11581-11595, 2016.
527 29. **Mohammadi MT**. Overproduction of nitric oxide intensifies brain infarction and cerebrovascular
528 damage through reduction of claudin-5 and ZO-1 expression in striatum of ischemic brain. *Pathology,*
529 *Research and Practice* 212: 959-964, 2016.
530 30. **Monzon CM, and Garvin JL**. Nitric oxide decreases the permselectivity of the paracellular
531 pathway in thick ascending limbs. *Hypertension* 65: 1245-1250, 2015.
532 31. **Ortiz PA, and Garvin JL**. Autocrine effects of nitric oxide on HCO(3)(-) transport by rat thick
533 ascending limb. *Kidney International* 58: 2069-2074, 2000.
534 32. **Ortiz PA, and Garvin JL**. Role of nitric oxide in the regulation of nephron transport. *American*
535 *Journal of Physiology Renal Physiology* 282: F777-784, 2002.
536 33. **Ortiz PA, Hong NJ, and Garvin JL**. NO decreases thick ascending limb chloride absorption by
537 reducing Na(+)-K(+)-2Cl(-) cotransporter activity. *American Journal of Physiology Renal Physiology* 281:
538 F819-825, 2001.
539 34. **Perez-Rojas JM, Kassem KM, Beierwaltes WH, Garvin JL, and Herrera M**. Nitric oxide produced
540 by endothelial nitric oxide synthase promotes diuresis. *American Journal of Physiology Regulatory,*
541 *Integrative and Comparative Physiology* 298: R1050-1055, 2010.
542 35. **Plato CF, Stoos BA, Wang D, and Garvin JL**. Endogenous nitric oxide inhibits chloride transport
543 in the thick ascending limb. *The American Journal of Physiology* 276: F159-163, 1999.
544 36. **Tain YL, Leu S, Wu KL, Lee WC, and Chan JY**. Melatonin prevents maternal fructose intake-
545 induced programmed hypertension in the offspring: roles of nitric oxide and arachidonic acid
546 metabolites. *Journal of Pineal Research* 57: 80-89, 2014.
547 37. **Trischitta F, Pidala P, and Faggio C**. Nitric oxide modulates ionic transport in the isolated
548 intestine of the eel, Anguilla anguilla. *Comp Biochem Phys A* 148: 368-373, 2007.

38. **Varela M, Herrera M, and Garvin JL**. Inhibition of Na-K-ATPase in thick ascending limbs by NO depends on O2- and is diminished by a high-salt diet. *American Journal of Physiology Renal Physiology* 287: F224-230, 2004.
39. **Wei Y, Babilonia E, Pedraza PL, Ferreri NR, and Wang WH**. Acute application of TNF stimulates apical 70-pS K+ channels in the thick ascending limb of rat kidney. *American Journal of Physiology Renal Physiology* 285: F491-497, 2003.
40. **Wen H, Watry DD, Marcondes MC, and Fox HS**. Selective decrease in paracellular conductance of tight junctions: role of the first extracellular domain of claudin-5. *Molecular and Cellular Biology* 24: 8408-8417, 2004.
41. **Winters CJ, Reeves WB, and Andreoli TE**. Cl- channels in basolateral renal medullary vesicles: V. Comparison of basolateral mTALH Cl- channels with apical Cl- channels from jejunum and trachea. *The Journal of Membrane Biology* 128: 27-39, 1992.
42. **Wu LL, Chiu HD, Peng WH, Lin BR, Lu KS, Lu YZ, and Yu LC**. Epithelial inducible nitric oxide synthase causes bacterial translocation by impairment of enterocytic tight junctions via intracellular signals of Rho-associated kinase and protein kinase C zeta. *Critical care medicine* 39: 2087-2098, 2011.
43. **Yu AS**. Claudins and the kidney. *Journal of the American Society of Nephrology : JASN* 26: 11-19, 2015.

Figure captions:

Fig 1. (A) Effect of L-arginine (L-arg) on specific transepithelial resistance (Rt; n=10); (B) The effect L-arg on specific Rt in the presence of the NO synthase inhibitor L-NAME (n=6). Individual experiments and means ± SEM are depicted.

Fig 2. (A) Effect of L-arginine (L-arg) on dilution potentials (n=9), (B) calculated P_{Na}^{+}/P_{Cl}^{-} and (C) paracellular P_{Na}^{+} and P_{Cl}^{-} in thick ascending limbs (n=50). Individual experiments and means ± SEM are depicted.

Fig 3. Effect of cGMP on specific transepithelial resistance (Rt) in thick ascending limbs (n=10). Individual experiments and means ± SEM are depicted.

Fig 4. (A) Effect of cGMP on dilution potentials (n=6), (B) calculated P_{Na}^{+}/P_{Cl}^{-} and (C) paracellular P_{Na}^{+} and P_{Cl}^{-} in thick ascending limbs (n=50). Individual experiments and means ± SEM are depicted.

Fig 5. Effect of NO on the luminal Na^+ concentration along the thick ascending limb as predicted by mathematical modeling. Each line illustrates the steady-state concentration of luminal Na^+ along the tubule.

Fig 6. Effect of NO on J_P along the thick ascending limb as predicted by mathematical modeling.

Fig 7. Effect of NO on (A) V_m, and its components (B) V_A and (C) $\alpha * V_P$ along the thick ascending limb as predicted by mathematical modeling. Each line indicates: effect on paracellular pathway only (dashed line), transcellular pathway only (blue line), both combined (green line) or control (solid black line).

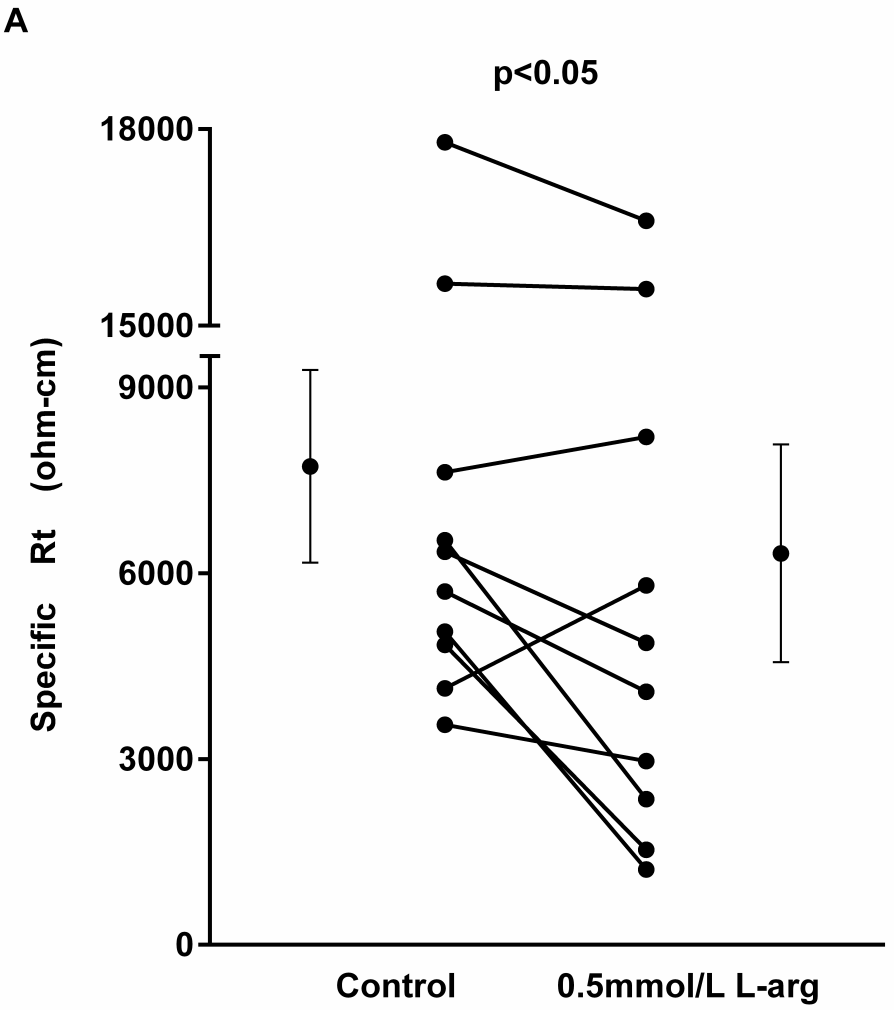
A
p<0.05
18000
15000
9000
6000
3000
0
Specific Rt (ohm-cm)
Control
0.5mmol/L L-arg

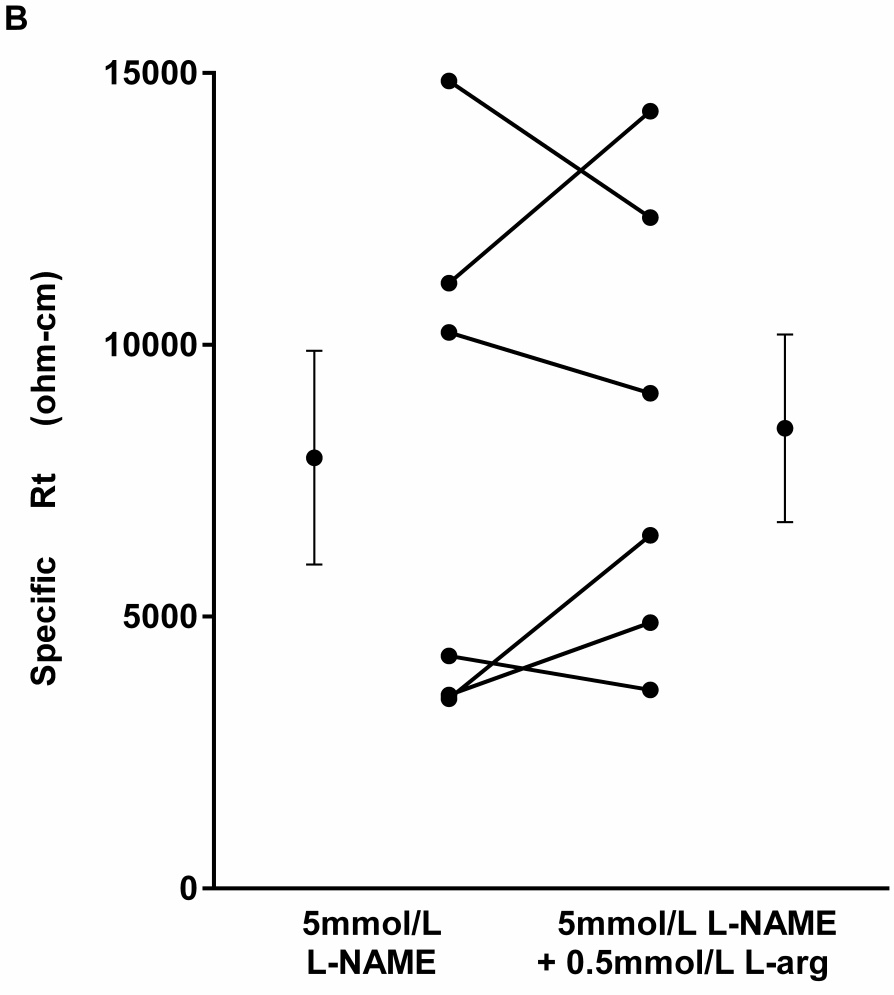
B
15000
10000
5000
0
Specific Rt (ohm-cm)
5mmol/L L-NAME
5mmol/L L-NAME + 0.5mmol/L L-arg

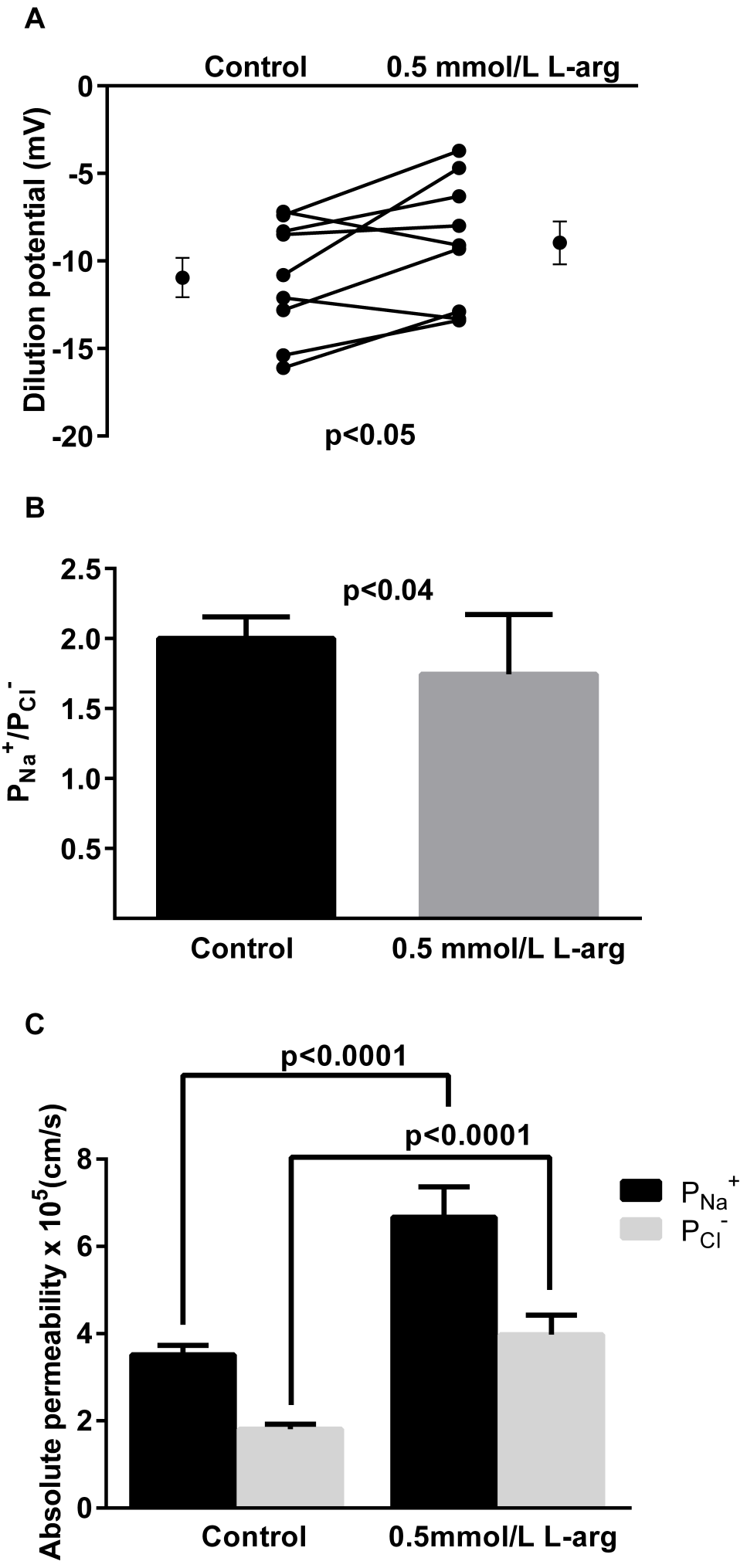
A
Control
0.5 mmol/L L-arg
0
-5
-10
-15
-20
Dilution potential (mV)
p<0.05
B
2.5
2.0
1.5
1.0
0.5
P_{Na}^{+}/P_{Cl}^{-}
p<0.04
Control
0.5 mmol/L L-arg
C
p<0.0001
p<0.0001
8
6
4
2
0
Absolute permeability x 10^5(cm/s)
P_{Na}^{+}
P_{Cl}^{-}
Control
0.5mmol/L L-arg

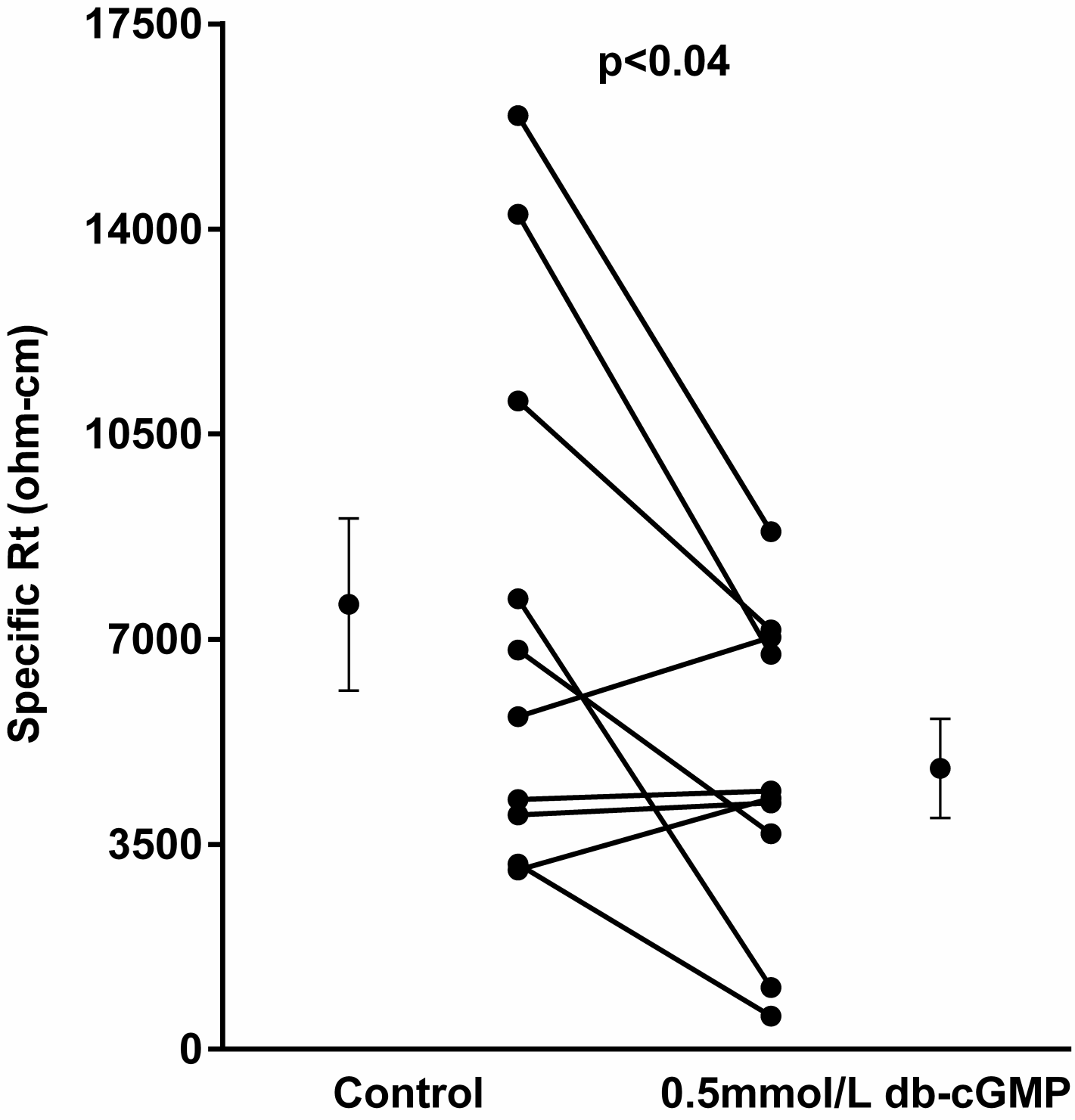
17500
14000
10500
7000
3500
0
Specific Rt (ohm-cm)
p<0.04
Control
0.5mmol/L db-cGMP

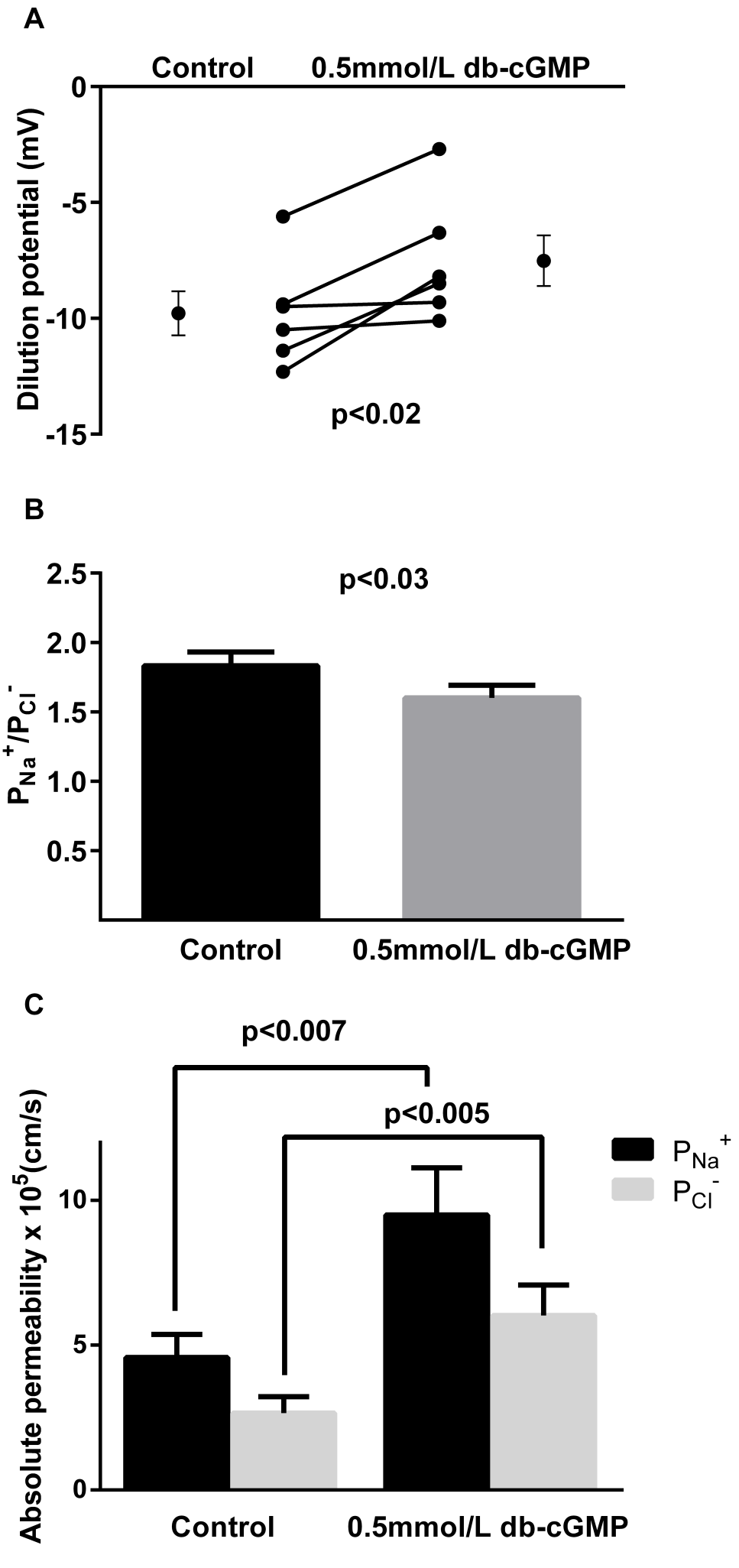
A
Control
0.5mmol/L db-cGMP
0
-5
-10
-15
Dilution potential (mV)
p<0.02
B
p<0.03
2.5
2.0
1.5
1.0
0.5
P_{Na}^{+}/P_{Cl}^{-}
Control
0.5mmol/L db-cGMP
C
p<0.007
p<0.005
10
5
0
Absolute permeability x 10^5(cm/s)
P_{Na}^{+}
P_{Cl}^{-}
Control
0.5mmol/L db-cGMP

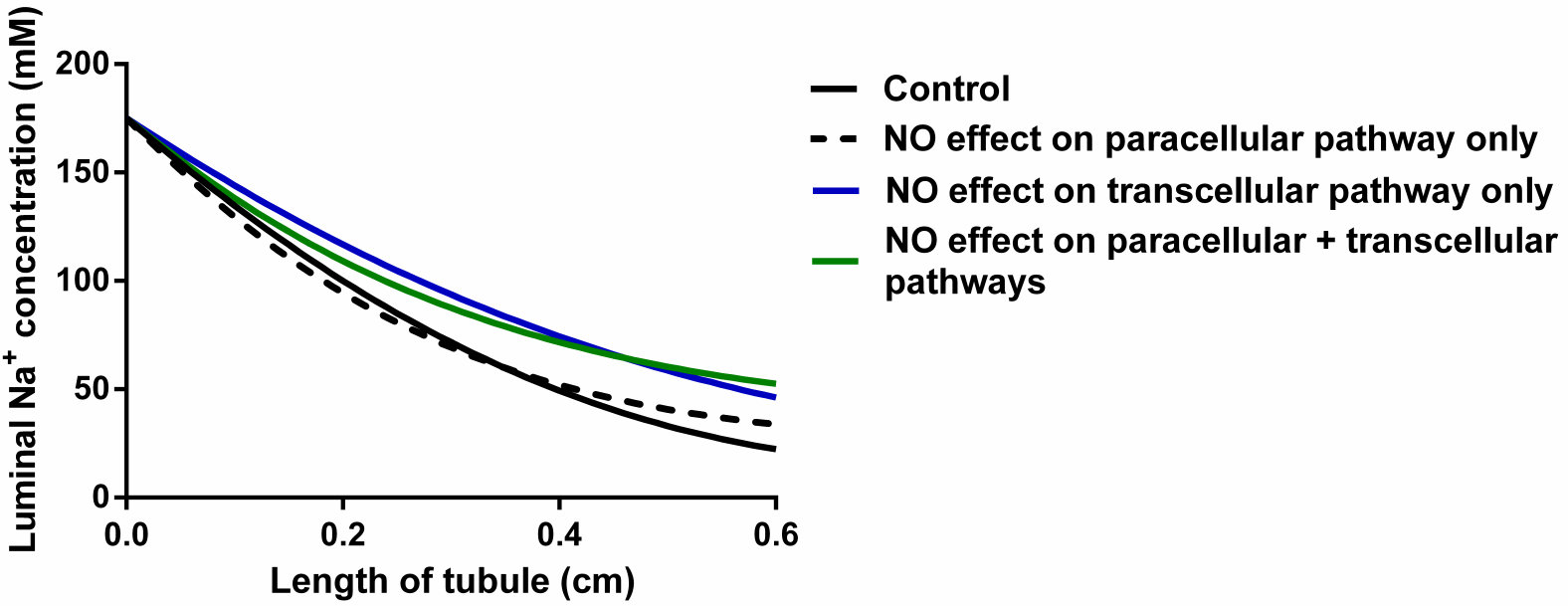
Luminal Na+ concentration (mM)
200
150
100
50
0
0.0
0.2
0.4
0.6
Length of tubule (cm)
Control
NO effect on paracellular pathway only
NO effect on transcellular pathway only
NO effect on paracellular + transcellular pathways

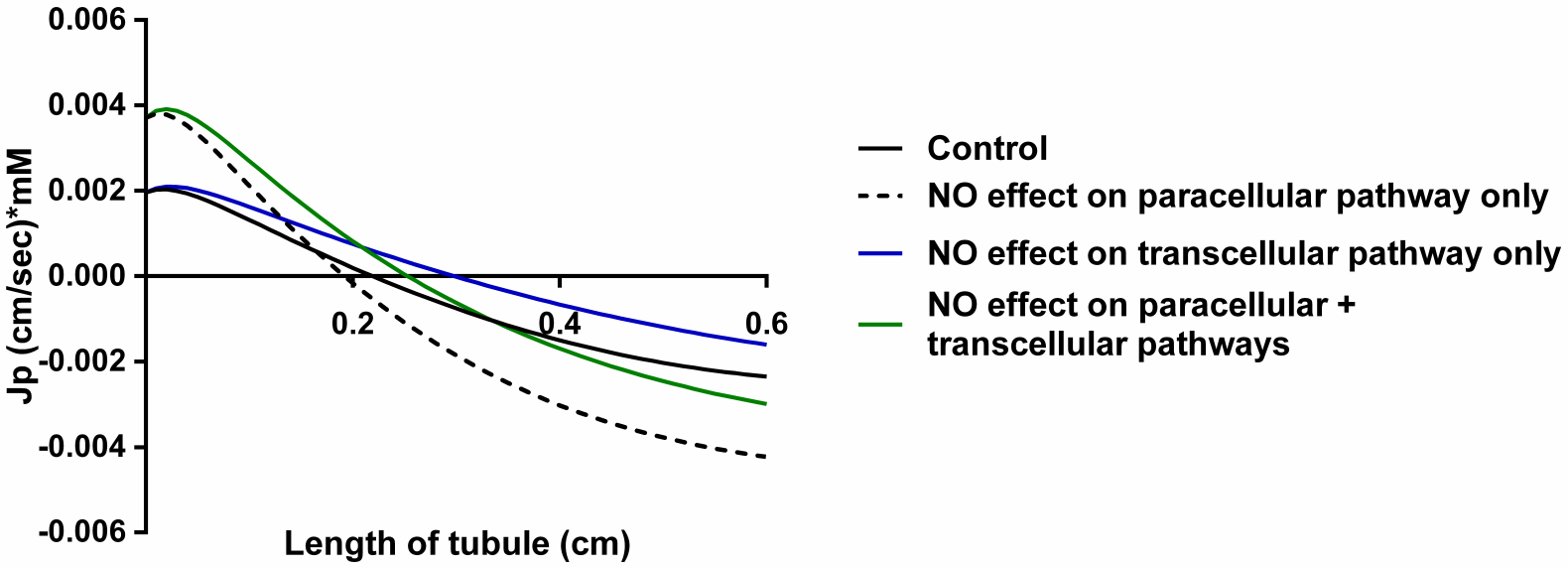
0.006
0.004
0.002
0.000
-0.002
-0.004
-0.006
Jp (cm/sec)*mM
0.2
0.4
0.6
Length of tubule (cm)
Control
NO effect on paracellular pathway only
NO effect on transcellular pathway only
NO effect on paracellular + transcellular pathways

A

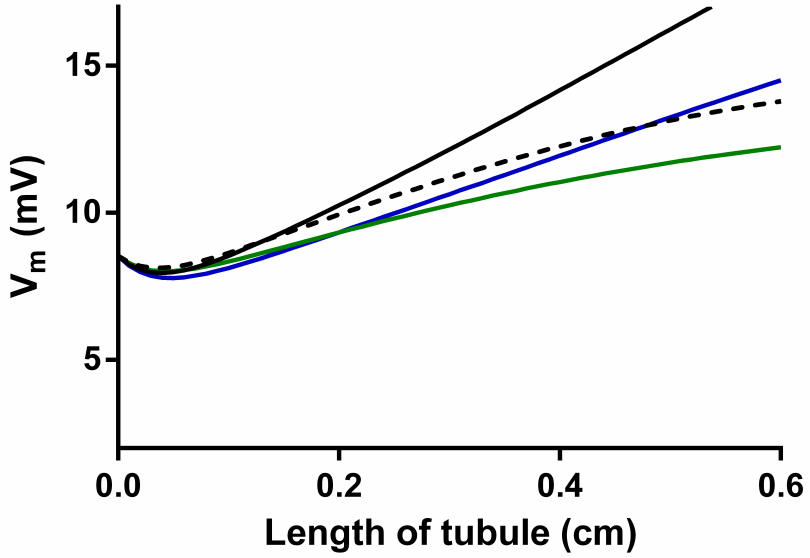
15
10
5
V_m (mV)
0.0
0.2
0.4
0.6
Length of tubule (cm)

B

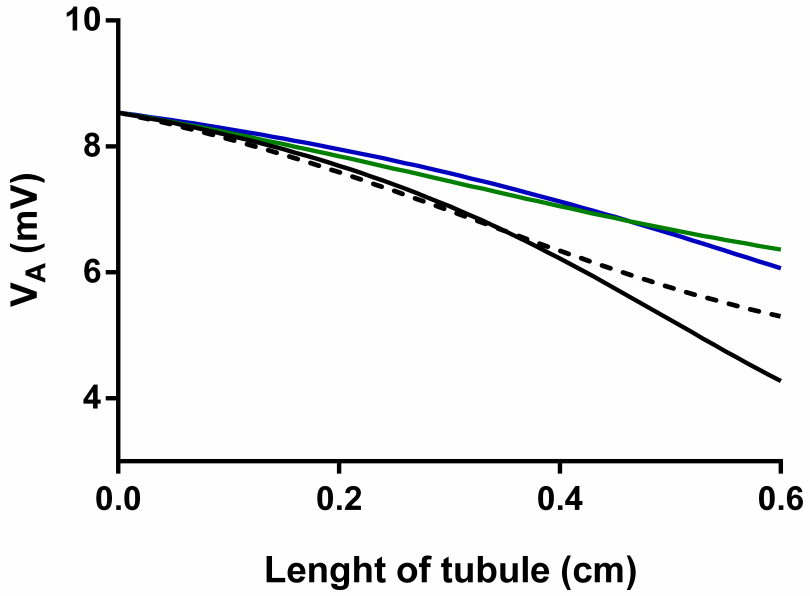
10
8
6
4
V_A (mV)
0.0
0.2
0.4
0.6
Lenght of tubule (cm)

C

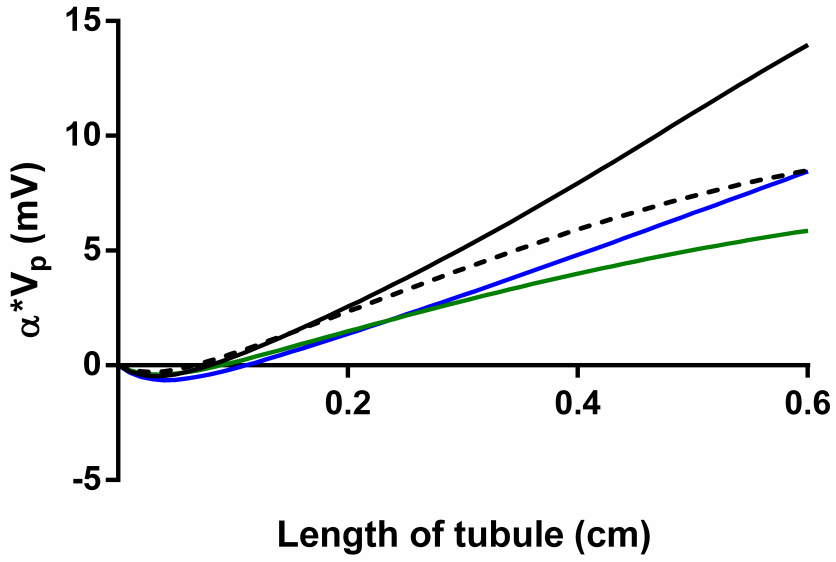
15
10
5
0
-5
α^*V_p (mV)
0.2
0.4
0.6
Length of tubule (cm)